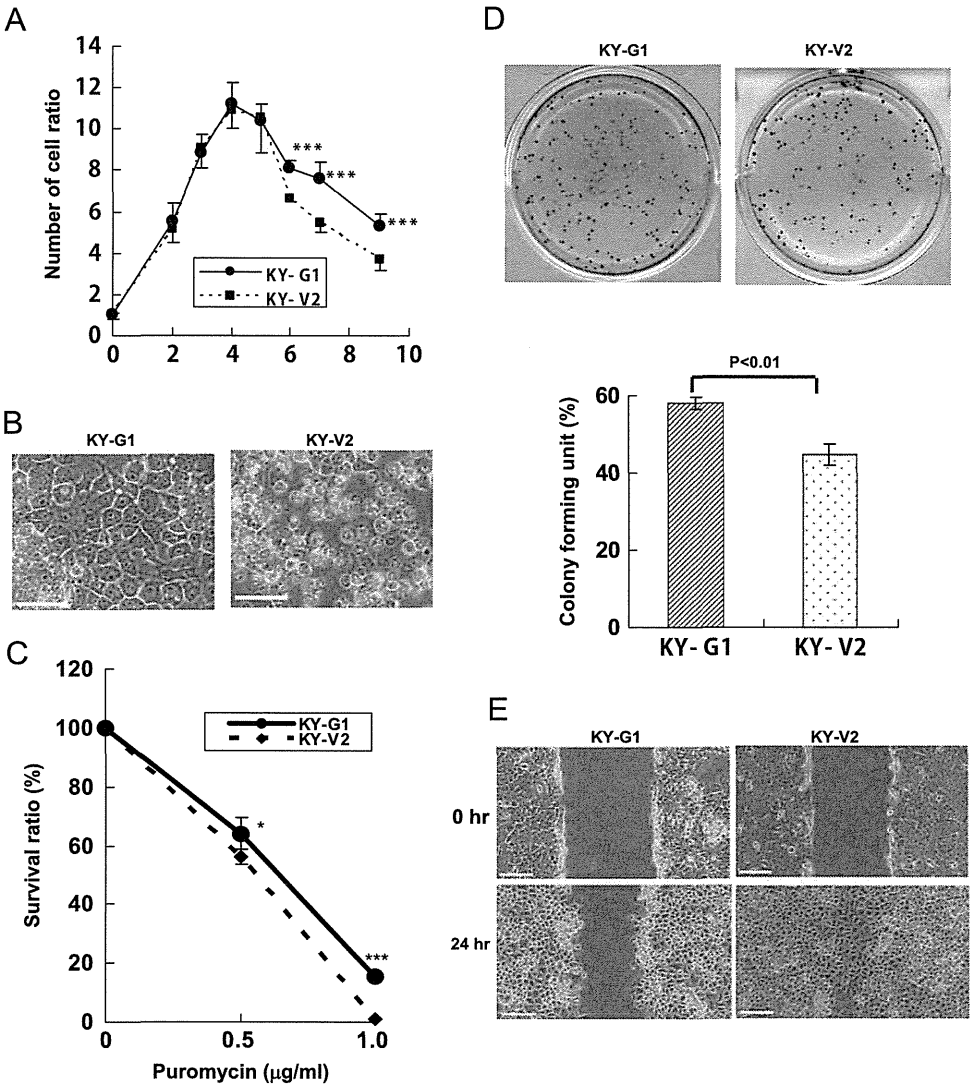

Fig. 2 – Characterization of LGR5-overexpressing clones. A: Growth and survival of KY-G1 and KY-V2 cells. High levels of LGR5 expression did not affect the growth rate of the cells; however, KY-G1 cells survived longer in overgrowth conditions. ***: $P<0.01$. B: Morphology of clones after 2 weeks of culture. (Bar, 100 μm) Viable cells were still observed in the KY-G1 culture, but few cells were alive in the KY-V2 culture. C: Resistance to cytotoxicity. Cells were treated with puromycin for 20 h, and cultured under soft agar medium. Cells with high expression of LGR5 were more resistant to the cytotoxic effect of puromycin. *: $P<0.05$. ***: $P<0.01$. D: Colony formation. Upper: 500 cells were cultured in soft agar plates for 2 weeks. Lower: quantitative assay of colony forming activity. Colony forming unit: ratio of colonies formed to number of cells inoculated (%). High levels of LGR5 expression enhanced colony formation. E: Motility assay. Confluent cell layers were scratched and photographed at 0 and 24 h. High levels of LGR5 expression inhibited cell motility. (Bar, 200 μm).

PLC/PRF/5 cells (Supplementary Fig. 2). When LGR5 mRNA was down-regulated with siRNA, the tight aggregated morphology of HepG2 cells was transformed to a loosely associated morphology. Some of the cells began to migrate away from the cell aggregates (Fig. 4A, upper column). The strongly staining cortical actins between the cells became extended filaments when expression of LGR5 was down-regulated (Fig. 4B, upper column). siRNA directed against LGR5 showed similar effects in PLC/PRF/5 cells (Fig. 4A and B, lower columns). The cortical actin between the cells became long, extended filaments. Down-regulation of LGR5 also increased cell motility. When HepG2 cells were treated with si585 or si662, scratched scars were repaired more rapidly than in cells treated with siControl (Fig. 5A, C). Similar results were obtained when PLC/PRF/5 cells were treated with siRNA directed against LGR5 (Fig. 5B, C).

Discussion

To determine the function of LGR5 in tumor cells, we carefully investigated cell clones containing a FLAG-tagged expression vector (LGR5-FL). The LGR-5 transfected clone (KY-G1) became rounded and formed aggregates when grown as an adherent culture. It formed spherical bodies when propagated in suspension culture, more resistance to cytocidal conditions, and showed decreased migratory activity. The Wnt signaling pathway is an

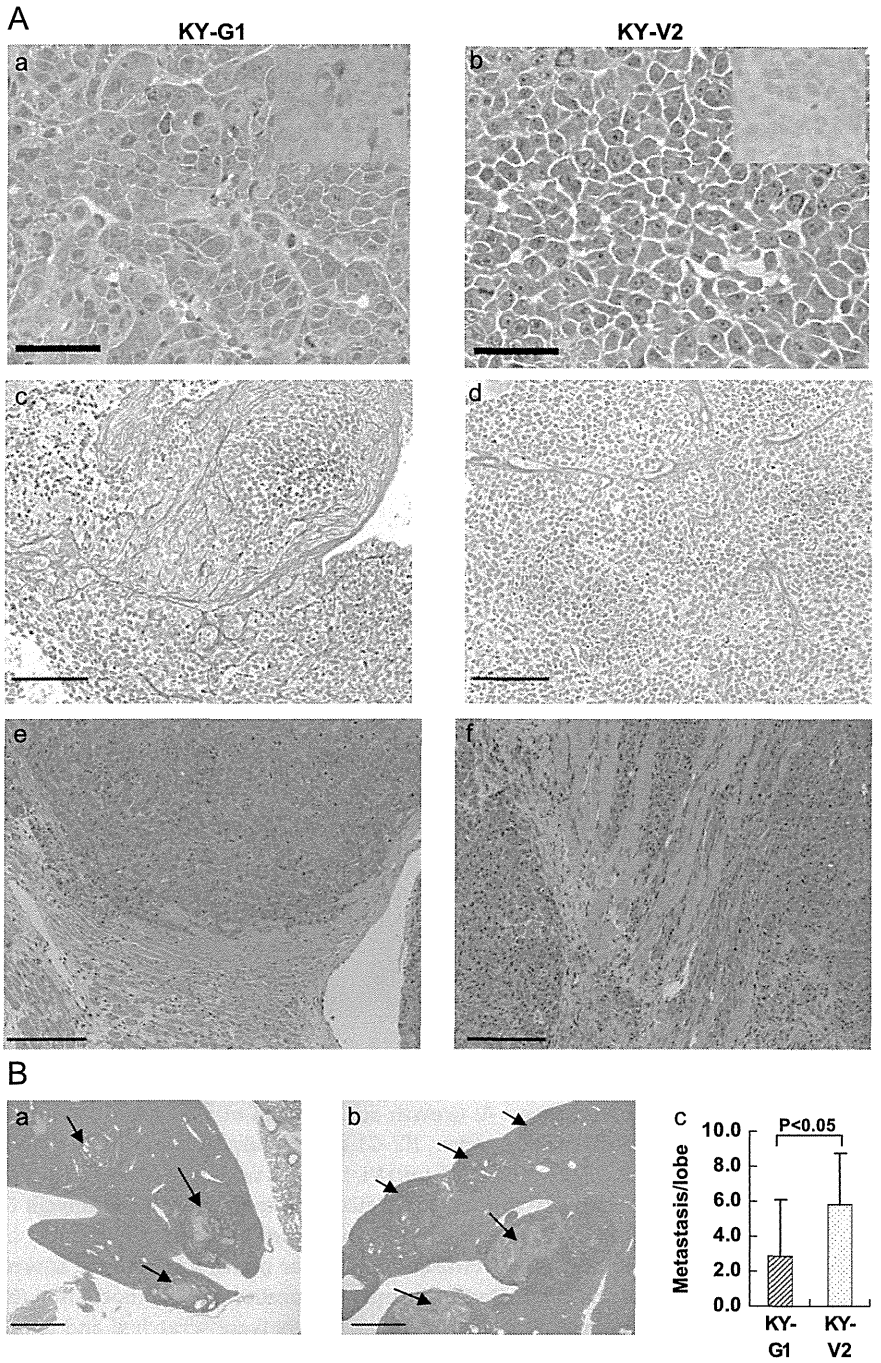

Fig. 3 – Histological analysis of tumors formed by KY-G1 or KY-V2 clones in the livers of NOG mice. A: KY-G1 (left) and KY-V2 (right) cells were transplanted into the subcapsular region of the livers of mice. Tumors were resected and thin sections were stained with HE (a, b. Bar, 100 μm)(e, f. Bar, 200 μm) or silver impregnation (c, d. Bar, 200 μm). Inserts show immunohistochemical staining with anti-FLAG antibody (a, b). B: KY-G1 (a) and KY-V2 (b) cells were transplanted into subcapsular region of the spleens of NOG mice. Tumors that formed in the livers were fixed and stained with HE (Bar 500 μm). Arrows show metastatic foci in the liver. The number of metastases was quantified (c). Tumors larger than 0.25 mm in diameter were counted. High levels of LGR5 expression inhibited metastasis to the liver.

important pathway for morphogenesis and maintaining the stemness of cells. Sphere formation, colony formation and resistance to cytotoxic drugs are important criteria for the stemness of cells. LGR5-overexpressing KY-G1 cells formed tightly packed spheres, with viable cells extending from the surface to the center when cultured under non-adherent conditions, whereas KY-V2 cells containing the empty vector formed loose, irregular spheres, and some cells in the central area showed signs of necrosis. KY-G1 cells were also more resistant to a cytocidal environment, survived longer under nutrient depletion conditions, and were more resistant to the cytocidal effect of puromycin. The differences between LGR5-transfected and vector-transfected cells were rather marginal, which may be affected by the

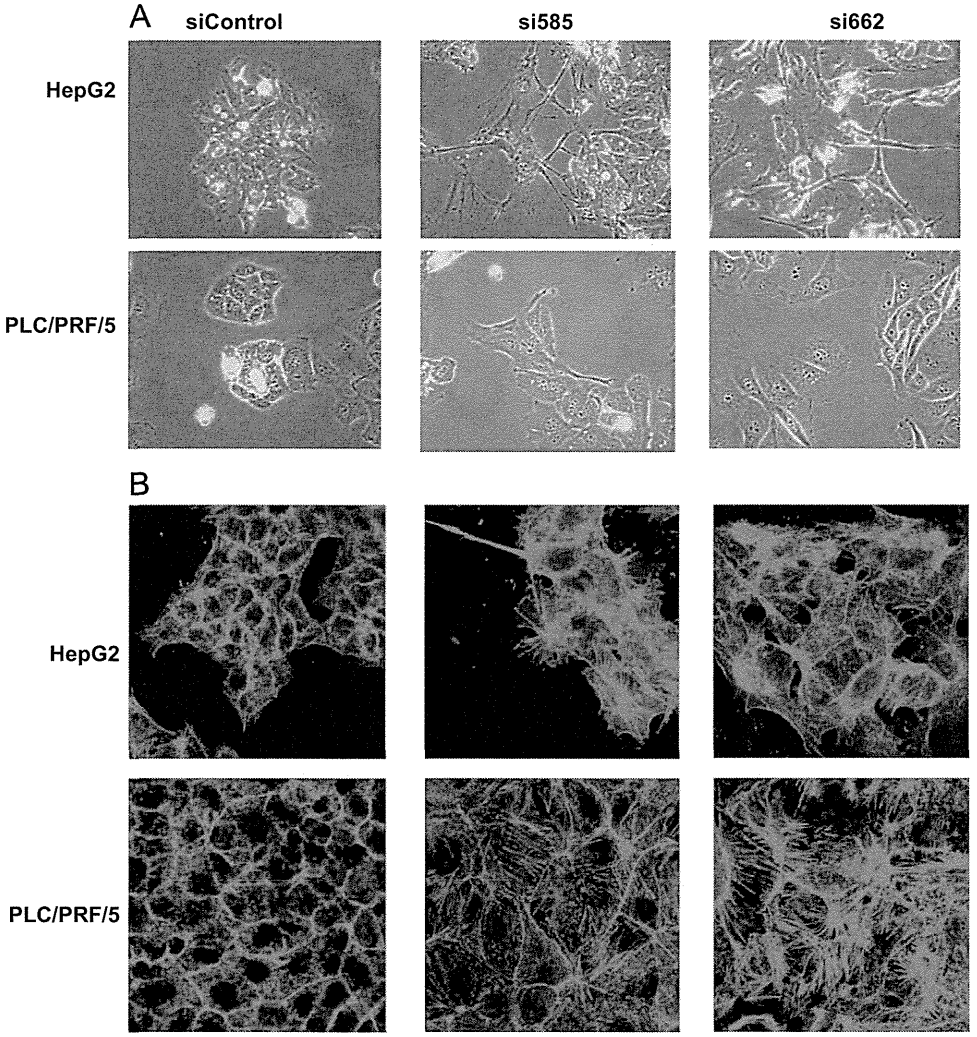

Fig. 4 – Down-regulation of LGR5 in HCC cell lines by treatment with siRNAs. HepG2 and PLC/PRF/5 cells were transfected with siControl, si585 or si662, and cultured for 2 days. A: Phase contrast microscopy. (×400) B: Immunofluorescent microscopy. Actin filaments were stained with phalloidin. (×400).

presence of substantial expression of LGR4 in parental KYN-2 cells. LGR4, LGR5, and LGR6 have homology with about 50% identity between each other at the amino acid level, and may compensate each other functions [18]. Since LGR4 is constitutively expressed in most kind of cells, we assumed that the results is more meaningful if we could obtain a difference between LGR5-overexpressing cells compared to the control empty vector cells, even though it is marginal. Moreover, we observed that parental KYN-2 cells had already reached the stage of anchorage-independent growth, while, a high level of LGR5 expression enhanced colony formation. This could be explained by high levels of LGR5 conferring resistance to cell death, and enhancing cell survival when they were scattered as single cells in the soft agar medium. KY-G1 cells aggregated and stacked up when cultured on the surface of the dishes, which consequently made them migrated slower than KY-V2 cells. These findings may explain why HCC is generally resistant to antitumor drugs used in chemotherapy. Many proteins related to the Wnt signaling pathway have been reported to modulate the actin–cytoskeleton structure. The frizzled/disheveled pathway controls the planar polarity of cells. Adenomatous polyposis coli (APC) protein is transported along microtubules, and regulates the cytoskeleton and cell migration [19]. β-catenin, a crucial transcription factor in the Wnt pathway, links E-cadherin with α-catenin to form firm adhesive junctions. LGR5, which is regarded as a target gene of the Wnt signaling pathway, quite possibly contributes to changes in cell morphology. Down-regulation of LGR5 in HepG2 and PLC/PRF/5 cells resulted in the cells acquiring a flat shape, with loss of cortical actin and migration of cells away from the aggregates. It also transformed HCC cells into a loosely associated morphology and increased cell motility. Reversely, high levels of LGR5 expression cells formed spherical shapes where most of the cells gathered intactly to the center. These results suggest that high levels of LGR5 expression affect epithelial cell morphology and confer some of the properties of stem cells on tumor cells.

To investigate the function of LGR5 in vivo, KY-G1 cells were orthotopically transplanted into NOG mice. KY-G1 cells formed nodular tumors typical of hepatocellular carcinomas, whereas the tumors formed by KY-V2 cells were diffuse and occasionally infiltrated into the contiguous tissues. Moreover, KY-V2 cells formed more micrometastases in the liver when implanted into the subcapsular region of the spleen. We previously categorized HCC cell lines into two groups; one highly metastatic and the

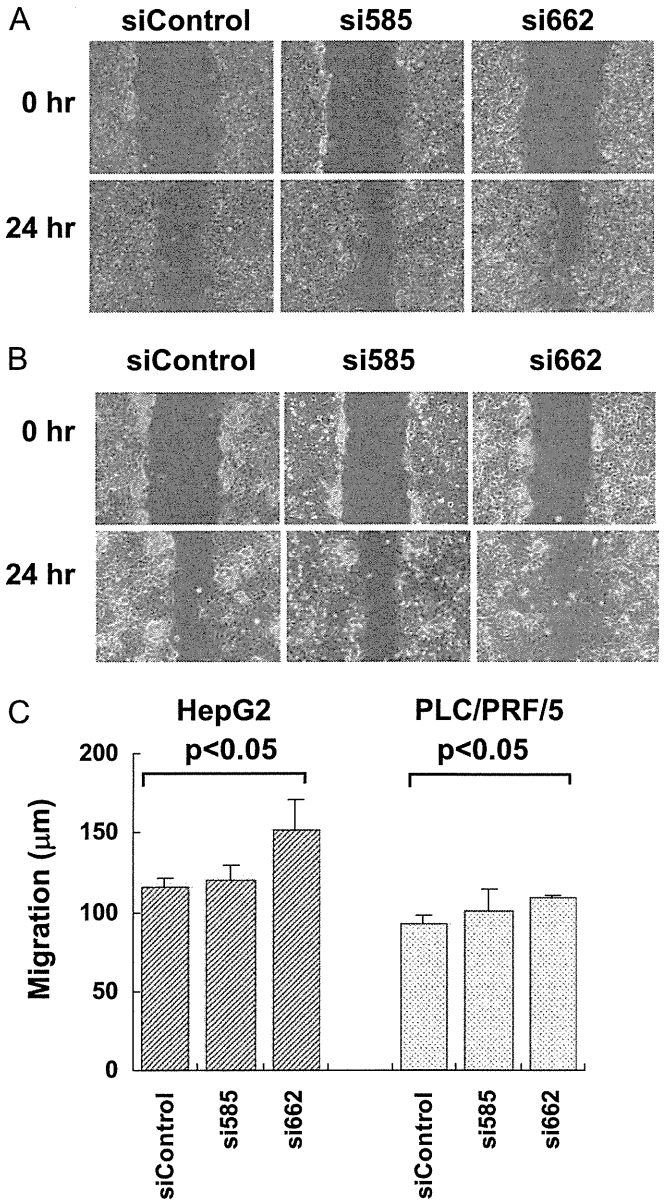

Fig. 5 – Motility of HCC cells after down-regulation of LGR5. Cells transfected with siControl, si585, or si662 were cultured for 2 days. Cell monolayers were scratched and photographed at 24 h. A: HepG2. B: PLC/PRF/5. C: Migration distance.

other non-metastatic [20]. It is quite interesting that KYN-2 and Li7 which express low levels of LGR5 were categorized as highly metastatic, whereas HepG2 and PLC/PRF/5 which express high levels of LGR5 were categorized in the non-metastatic group. Our previous clinicopathological study also showed that overexpression of LGR5 was more frequent in HCC with well to moderate differentiation compared with poorly differentiated HCC, although the difference was not statistically significant [6]. Here, we showed that the level of LGR5 expression in HCC cells affected the morphology of the tumors and their metastatic properties. Our present findings showed similar analogies with the features of clinical HCC regarding LGR5 expression. There is a possibility that high levels of LGR5 expression in HCC be the cause of the typical morphological and biological characteristics of some subclasses of HCC.

We observed similar morphological changes from various kinds of tumor cells by overexpression or down-regulation of LGR5 (unpublished data). One recent report showed that suppression of LGR5 expression in colorectal cancer cells enhanced tumor formation with increased cell motility, while cells overexpressing LGR5 tend to grow in 'colonies' with tight cell-to-cells contact and had reduction in cell motility [10]. Their observations on morphological changes and some other biological functions of LGR5 are mostly in agreement with our results, although the background of cell linage is different. Therefore, we think that our observations from the present study are not specific only to HCC, but are more generally applicable to the certain types of tumors.

Since the ligand of LGR5 has long been unknown, LGR5 has been categorized as an orphan receptor. Recently, R-spondins (Roof plate-specific Spondin, RSPOs) has been reported as ligands of LGR5 and required for sufficient activation of Wnt/β-catenin signaling [11,12,14]. To know whether overexpression of LGR5 affects the expression of RSPOs and potentiate Wnt/β-catenin signaling, we additionally measured expression of R-Spondin 1 (RSPO1) mRNA, and analyzed Wnt/β-catenin signaling level with

TOPflash/FOPflash TCF-luciferase reporter system (Supplementary Fig. 3). The expression of RSPO1 was not dependent on or related to in parallel with LGR5 expression. In HCC cell lines with high levels of LGR5 expression (HepG2), a high expression level of RSPO1 was observed. However, RSPO1 was also highly expressed in KIM 1 with low levels of LGR5. Also in LGR5-overexpressing cell (KY-G1, KY-S1) and empty vector cell (KY-V2, KY-V3), the expression of RSPO1 was not affected. In colorectal cell lines, expression level of RSPO1 was low in high LGR5 expressed cells, LoVo, whereas it was high in low expressed LGR5 cells, HCT116. We found that TOPFLASH/FOPFLASH ratio in LGR5-overexpressing KY-G1 cells was not significantly different from the vector-transfected clone. Furthermore, nuclear accumulation of β-catenin which is usually accompanied with activated Wnt signaling pathway was not detected in the LGR5-overexpressing clone (Fig. 1H). These results suggest that morphological changes and some other properties given from aberrant expression of LGR5 in tumor cells are not likely regulated by augmented Wnt signaling through R-spondin/LGR5 signaling pathway.

In this study we have shown that high levels of LGR5 expression confer cells with some of the properties of stem cells, including sphere formation and enhanced survival. In addition, high levels of LGR5 expression in vivo transformed tumors from a diffuse to a more nodular phenotype and from a metastatic to a less metastatic phenotype. These rather complicated biological roles of LGR5 may explain some of the complexity of human cancers, and further detailed studies of LGR5 would shed light on its biological functions and on the development of effective treatment strategies for cancer.

Disclosure statement

The authors have no conflict of interest.

Acknowledgments

We thank H. Suzuki, Y. Hashimoto and H. Abe for their excellent technical assistance. This work was supported by a Grant-in-Aid for Scientific Research (B) from the Ministry of Education, Culture, Sports, Science and Technology of Japan; and Third Term Comprehensive 10-Years Strategy for Cancer Control from the Ministry of Health, Labor and Welfare of Japan to M.S.

Appendix A. Supporting information

Supplementary data associated with this article can be found in the online version at http://dx.doi.org/10.1016/j.yexcr.2012.10.011.

REFERENCES

[1] H. Morita, S. Mazerbourg, D.M. Bouley, C.W. Luo, K. Kawamura, Y. Kuwabara, H. Baribault, H. Tian, A.J. Hsueh, Neonatal lethality of LGR5 null mice is associated with ankyloglossia and gastrointestinal distension, Mol. Cell. Biol. 24 (2004) 9736–9743.

[2] M.I. Garcia, M. Ghiani, A. Lefort, F. Libert, S. Strollo, G. Vassart, LGR5 deficiency deregulates Wnt signaling and leads to precocious Paneth cell differentiation in the fetal intestine, Dev. Biol. 331 (2009) 58–67.

[3] N. Barker, J.H. van Es, J. Kuipers, P. Kujala, M. van den Born, M. Cozijnsen, A. Haegebarth, J. Korving, H. Begthel, P.J. Peters, H. Clevers, Identification of stem cells in small intestine and colon by marker gene Lgr5, Nature 449 (2007) 1003–1007.

[4] N. Barker, R.A. Ridgway, J.H. van Es, M. van de Wetering, H. Begthel, M. van den Born, E. Danenberg, A.R. Clarke, O.J. Sansom, H. Clevers, Crypt stem cells as the cells-of-origin of intestinal cancer, Nature 457 (2009) 608–611.

[5] V. Jaks, N. Barker, M. Kasper, J.H. van Es, H.J. Snippert, H. Clevers, R. Toftgard, Lgr5 marks cycling, yet long-lived, hair follicle stem cells, Nat. Genet. 40 (2008) 1291–1299.

[6] Y. Yamamoto, M. Sakamoto, G. Fujii, H. Tsuiji, K. Kenetaka, M. Asaka, S. Hirohashi, Overexpression of orphan G-protein-coupled receptor, Gpr49, in human hepatocellular carcinomas with beta-catenin mutations, Hepatology 37 (2003) 528–533.

[7] K. Tanese, M. Fukuma, T. Yamada, T. Mori, T. Yoshikawa, W. Watanabe, A. Ishiko, M. Amagai, T. Nishikawa, M. Sakamoto, G-protein-coupled receptor GPR49 is up-regulated in basal cell carcinoma and promotes cell proliferation and tumor formation, Am. J. Pathol. 173 (2008) 835–843.

[8] T. McClanahan, S. Koseoglu, K. Smith, J. Grein, E. Gustafson, S. Black, P. Kirschmeier, A.A. Samatar, Identification of overexpression of orphan G protein-coupled receptor GPR49 in human colon and ovarian primary tumors, Cancer Biol. Ther. 5 (2006) 419–426.

[9] H. Uchida, K. Yamazaki, M. Fukuma, T. Yamada, T. Hayashida, H. Hasegawa, M. Kitajima, Y. Kitagawa, M. Sakamoto, Overexpression of leucine-rich repeat-containing G protein-coupled receptor 5 in colorectal cancer. Cancer Science 101 (2010) 1731–1737.

[10] F. Walker, H.H. Zhang, A. Odorizzi, A.W. Burgess, LGR5 is a negative regulator of tumourigenicity, antagonizes Wnt signalling and regulates cell adhesion in colorectal cancer cell lines. PloS one 6 (2011) e22733.

[11] W. de Lau, N. Barker, T.Y. Low, B.K. Koo, V.S. Li, H. Teunissen, P. Kujala, A. Haegebarth, P.J. Peters, M. van de Wetering, D.E. Stange, J.E. van Es, D. Guardavaccaro, R.B. Schasfoort, Y. Mohri, K. Nishimori, S. Mohammed, A.J. Heck, H. Clevers, Lgr5 homologues associate with Wnt receptors and mediate R-spondin signalling. Nature 476 (2011) 293–297.

[12] K.S. Carmon, Q. Lin, X. Gong, A. Thomas, Q. Liu, LGR5 interacts and cointernalizes with Wnt receptors to modulate Wnt/beta-catenin signaling. Molecular and Cellular Biology 32 (2012) 2054–2064.

[13] Y. Komiya, R. Habas, Wnt signal transduction pathways, Organogenesis 4 (2008) 68–75.

[14] A. Glinka, C. Dolde, N. Kirsch, Y.L. Huang, O. Kazanskaya, D. Ingelfinger, M. Boutros, C.M. Cruciat, C. Niehrs, LGR4 and LGR5 are R-spondin receptors mediating Wnt/beta-catenin and Wnt/PCP signalling. EMBO Reports 12 (2011) 1055–1061.

[15] T. Reya, S.J. Morrison, M.F. Clarke, I.L. Weissman, Stem cells, cancer, and cancer stem cells, Nature 414 (2001) 105–111.

[16] R. Pardal, M.F. Clarke, S.J. Morrison, Applying the principles of stem-cell biology to cancer, Nature Rev. 3 (2003) 895–902.

[17] N. Sato, L. Meijer, L. Skaltsounis, P. Greengard, A.H. Brivanlou, Maintenance of pluripotency in human and mouse embryonic stem cells through activation of Wnt signaling by a pharmacological GSK-3-specific inhibitor, Nature Med. 10 (2004) 55–63.

[18] X. Gong, K.S. Carmon, Q. Lin, A. Thomas, J. Yi, Q. Liu, LGR6 is a high affinity receptor of R-spondins and potentially functions as a tumor suppressor. PloS one 7 (2012) e37137.

[19] Y. Mimori-Kiyosue, C. Matsui, H. Sasaki, S. Tsukita, Adenomatous polyposis coli (APC) protein regulates epithelial cell migration and morphogenesis via PDZ domain-based interactions with plasma membranes, Genes Cells 12 (2007) 219–233.

[20] M. Chuma, M. Sakamoto, J. Yasuda, G. Fujii, K. Nakanishi, A. Tsuchiya, T. Ohta, M. Asaka, S. Hirohashi, Overexpression of cortactin is involved in motility and metastasis of hepatocellular carcinoma, J. hepatology 41 (2004) 629–636.

Hepatology Research

Hepatology Research 2013 doi: 10.1111/hepr.12254

Original Article

Hepatic oxidative stress in ovariectomized transgenic mice expressing the hepatitis C virus polyprotein is augmented through suppression of adenosine monophosphate-activated protein kinase/proliferator-activated receptor gamma co-activator 1 alpha signaling

Yasuyuki Tomiyama, Sohji Nishina, Yuichi Hara, Tomoya Kawase and Keisuke Hino

Department of Hepatology and Pancreatology, Kawasaki Medical School, Kurashiki, Japan

Aim: Oxidative stress plays an important role in hepatocarcinogenesis of hepatitis C virus (HCV)-related chronic liver diseases. Despite the evidence of an increased proportion of females among elderly patients with HCV-related hepatocellular carcinoma (HCC), it remains unknown whether HCV augments hepatic oxidative stress in postmenopausal women. The aim of this study was to determine whether oxidative stress was augmented in ovariectomized (OVX) transgenic mice expressing the HCV polyprotein and to investigate its underlying mechanisms.

Methods: OVX and sham-operated female transgenic mice expressing the HCV polyprotein and non-transgenic littermates were assessed for the production of reactive oxygen species (ROS), expression of inflammatory cytokines and antioxidant potential in the liver.

Results: Compared with OVX non-transgenic mice, OVX transgenic mice showed marked hepatic steatosis and ROS production without increased induction of inflammatory cytokines, but there was no increase in ROS-detoxifying enzymes such as superoxide dismutase 2 and glutathione peroxidase 1. In accordance with these results, OVX transgenic mice showed less activation of peroxisome proliferator-activated receptor-γ co-activator-1α (PGC-1α), which is required for the induction of ROS-detoxifying enzymes, and no activation of adenosine monophosphate-activated protein kinase-α (AMPKα), which regulates the activity of PGC-1α.

Conclusion: Our study demonstrated that hepatic oxidative stress was augmented in OVX transgenic mice expressing the HCV polyprotein by attenuation of antioxidant potential through inhibition of AMPK/PGC-1α signaling. These results may account in part for the mechanisms by which HCV-infected women are at high risk for HCC development when some period has passed after menopause.

Key words: antioxidant potential, glutathione peroxidase, reactive oxygen species, superoxide dismutase

INTRODUCTION

PERSISTENT HEPATITIS C virus (HCV) infection is a major risk factor for the development of hepatocellular carcinoma (HCC) in Japan. Approximately 70% of Japanese HCC patients are currently diagnosed with HCV-associated cirrhosis or chronic hepatitis C.[1] Nevertheless, the mechanisms underlying HCV-associated hepatocarcinogenesis are incompletely understood. Notably, there is sex disparity in HCC development, that is, male sex has been demonstrated to be an independent risk factor associated with HCC development.[2–4] It is proposed that estrogen-mediated inhibition of interleukin (IL)-6 production by Kupffer cells reduces the HCC risk in females.[5] In addition, the proportion of females among elderly patients with HCV-related HCC has recently increased in Japan.[6] These results suggest that menopause may be a risk factor associated with HCC development in female patients with HCV infection.

Numerous studies have shown that oxidative stress is present in chronic hepatitis C to a greater degree than in other inflammatory disease,[7,8] and is related to

Correspondence: Professor Keisuke Hino, Department of Hepatology and Pancreatology, Kawasaki Medical School, 577 Matsushima, Kurashiki, Okayama 701-0192, Japan. Email: khino@med.kawasaki-m.ac.jp

Received 9 September 2013; revision 24 September 2013; accepted 30 September 2013.

hepatocarcinogenesis in HCV-associated chronic liver diseases.[9,10] We have previously demonstrated that transgenic mice expressing the HCV polyprotein develop liver tumors including HCC, in connection with oxidative stress induced by HCV and iron overload.[11] Interestingly, such hepatocarcinogenesis was observed only in male transgenic mice, suggesting that females are resistant to oxidative stress in these transgenic mice. On the other hand, it is reported that ovariectomy increases nicotinamide adenine dinucleotide phosphate (NADPH) oxidase activity[12] and decreases mitochondrial-reduced glutathione levels in rats.[13] However, it remains unknown how HCV affects ovariectomy-induced oxidative stress. Investigation of this issue may provide a clue for understanding why the incidence of HCC increases in elderly postmenopausal women with HCV infection. The aim of this study was to determine whether HCV proteins amplify oxidative stress induced by ovariectomy and to investigate the mechanisms underlying this.

METHODS

Animals

CONTAINING THE FULL-LENGTH polyprotein-coding region under the control of the murine albumin promoter/enhancer, the transgene pAlbSVPA-HCV has been described in detail.[14,15] Of the four transgenic lineages with evidence of RNA transcription of the full-length HCV-N open reading frame (FL-N), the FL-N/35 lineage proved capable of breeding in large numbers. There is no inflammation in the transgenic liver.[15]

Experimental design

Female FL-N/35 transgenic mice and their normal female C57BL/6 littermates were anesthetized for surgery and underwent either a bilateral ovariectomy or sham operation at the age of 4–6 weeks. We studied ovariectomized (OVX) transgenic mice ($n = 5$), sham-operated transgenic mice ($n = 5$), OVX non-transgenic mice ($n = 5$) and sham-operated non-transgenic mice ($n = 5$). These mice were fed a normal rodent diet, bred, maintained, and killed by i.p. injection of 10% pentobarbital sodium preceded by 20-h fasting at the age of 24 weeks. All experimental protocols and animal maintenance procedures used in this study were approved by the Ethics Review Committee for Animal Experimentation of Kawasaki Medical School.

Histological procedures

A portion of liver tissue was immediately snap-frozen in liquid nitrogen for determination of the hepatic triglyceride concentration. The remaining liver tissue was fixed in 4% paraformaldehyde in phosphate-buffered saline and embedded in paraffin for histological analyses. Liver sections were stained with hematoxylin–eosin.

Serum leptin concentration

The serum leptin level was measured using a Rat Leptin Elisa kit (Morinaga Institute of Biological Science, Yokohama, Japan) according to the manufacturer's instructions.

Hepatic triglyceride content

Lipids were extracted from the homogenized liver tissue by the method of Bligh and Dyer.[16] The triglyceride level was measured with a TGE-test Wako kit (Wako Pure Chemicals, Tokyo, Japan), according to the manufacturer's instructions. Protein concentrations in liver were determined by the method of Lowry *et al.*,[17] using a DC protein assay kit (Bio-Rad Laboratories, Hercules, CA, USA).

In situ detection of reactive oxygen species (ROS)

In situ ROS production in the liver was assessed by staining with dihydroethidium, as described previously.[18] In the presence of ROS, dihydroethidium (Invitrogen, Carlsbad, CA, USA) is oxidized to ethidium bromide and stains nuclei bright red by intercalating with the DNA.[19] Fluorescence intensity was quantified using National Institutes of Health image analysis software for 3 randomly selected areas of digital images for each mouse.

Hepatic iron content

Hepatic iron content was measured by atomic absorption spectrometry, as described previously,[11] and expressed as micrograms Fe per gram of tissue (wet weight).

Derivatives of reactive oxygen metabolites (dROM) and biological antioxidant potential (BAP)

The levels of dROM and BAP were measured using a Free Radical Elective Evaluator (Wismerll, Tokyo, Japan), as described previously.[20] Measurement of dROM is based on the ability of the transition metal ions to catalyze the formation of alkoxy and peroxy radicals from hydroper-

oxides present in serum. The results are expressed in conventional units as Carrtelli units (U.CARR), where 1 U.CARR corresponds to 0.8 mg/L H_2O_2. Measurement of BAP is based on the ability of antioxidants to reduce ferric (F^{3+}) ions to ferrous (Fe^{2+}) ions.

RNA isolation and real-time reverse transcription polymerase chain reaction (RT–PCR)

Total RNA was isolated using an RNeasy mini kit (QIAGEN, Hilden, Germany) and reverse-transcribed into cDNA by using a Superscript III reverse transcription kit (Invitrogen). The PCR reactions were run in the ABI Prism 7700 sequence detection system (Applied Biosystems, Foster, CA, USA). The levels of mRNA were determined using cataloged primers (Applied Biosystems) for mice (tumor necrosis factor [TNF]-α, Mm00443258_m1; IL-1β, Mm00434228_m1; IL-6, Mm00446190_m1; HAMP [gene encoding hepcidin], Mm00519025_mL; superoxide dismutase 2 [SOD2], Mm01313000_m1; glutathione peroxidase 1 [GPx1], Mm00656767_g1; and sirtuin 3 [SIRT3], Mm00452131_m1). Expression of these genes was normalized to expression of glyceraldehyde 3-phosphate dehydrogenase mRNA (GAPDH, Mm99999915_g1).

Isolation of mitochondria and nuclear fraction

Mitochondrial extraction from liver tissue was performed using a Qproteome Mitochondrial Isolation kit (QIAGEN) according to the manufacturer's instructions. The nuclear fraction from liver tissue was prepared using a Nuclear Extraction kit (Panomics, Fremont, CA, USA) according to the manufacturer's instructions.

Immunoblotting

Liver lysates and the mitochondrial and nuclear fractions from liver were separated by sodium dodecylsulfate polyacrylamide gel electrophoresis. The proteins were transferred to polyvinylidene difluoride membranes (Millipore, Bradford, MA, USA), blocked overnight at 4°C with 5% skim milk and 0.1% Tween-20 in Tris-buffered saline, and subsequently incubated for 1 h at room temperature with goat antihuman SOD2 antibody (Santa Cruz Biotechnology, Santa Cruz, CA, USA), rabbit antihuman GPx1 antibody (Abcam, Cambridge, MA, USA), rabbit antihuman SIRT3 antibody (Abcam), rabbit antihuman peroxisome proliferator-activated receptor-γ co-activator-1α (PGC-1α) antibody (Abcam), rabbit antihuman adenosine monophosphate-activated protein kinase-α (AMPKα) antibody (Cell Signaling Technology, Boston, MA, USA), rabbit antihuman phospho-AMPKα (Thr172) antibody (Cell Signaling Technology), rabbit antihuman mitochondrial heat shock protein 70 antibody (HSP70; Thermo Scientific, Rockford, IL, USA), rabbit antihuman β-actin antibody (Cell Signaling Technology) or rabbit antimouse lamin B1 antibody (Abcam). The membranes were washed and incubated with horseradish peroxidase (HRP)-conjugated donkey antigoat immunoglobulin (Ig)G (Santa Cruz Biotechnology) or HRP-conjugated donkey antirabbit IgG (GE Healthcare Life Sciences, Pittsburgh, PA, USA).

Statistical analysis

Quantitative values are expressed as mean ± standard deviation. Two groups among multiple groups were compared by the rank-based Kruskal–Wallis ANOVA test followed by Scheffé's test. The statistical significance of correlation was determined by the use of simple regression analysis. $P < 0.05$ was considered to be significant.

RESULTS

Ovariectomy enhanced hepatic steatosis in FL-N/35 transgenic mice

AS CONFIRMATION OF successful ovariectomy-induced suppression of endogenous estrogen production, the uterine weight of OVX mice was significantly decreased compared with that of sham-operated mice (Table 1). Dietary intake, bodyweight, liver weight and serum leptin levels were significantly greater in OVX mice than in sham-operated mice regardless of whether they were transgenic or non-transgenic (Table 1). Interestingly, the serum alanine aminotransferase (ALT) level was significantly higher in OVX transgenic mice than in mice in the other three groups, but the levels were comparable in OVX non-transgenic and sham-operated non-transgenic mice (Table 1). To determine why OVX transgenic mice have a higher ALT level, we investigated the liver histology of the mice in the four groups (OVX transgenic, sham-operated transgenic, OVX non-transgenic and sham-operated non-transgenic mice). In contrast to the mild to moderate degree of hepatic steatosis noted in OVX non-transgenic mice and sham-operated transgenic mice, OVX transgenic mice developed severe hepatic steatosis (Fig. 1a) without infiltration of inflammatory mononuclear cells. Hepatic triglyceride content was measured to quantify the degree of steatosis. The triglyceride content was significantly greater in OVX transgenic mice than in mice in the other three groups (Fig. 1b), which was consistent with the

Table 1 Body, liver and uterus weight and serum biochemical parameters

Body, liver, and uterus weight and serum biochemical parameters	Non-transgenic		Transgenic	
	Sham-operated	OVX	Sham-operated	OVX
Bodyweight (g)	21.5 ± 1.2	30.7 ± 4.9*	27.7 ± 4.6	34.2 ± 3.8**
Liver weight (g)	0.86 ± 0.075	1.09 ± 0.236*	0.90 ± 0.102	1.18 ± 0.156**
Ratio of liver to bodyweight	0.038 ± 0.037	0.035 ± 0.003	0.031 ± 0.002	0.034 ± 0.006
Uterus weight (g)	0.08 ± 0.01	0.01 ± 0.02*	0.09 ± 0.01	0.01 ± 0.01**
Total dietary intake (g)	337 ± 24	429 ± 13*	368 ± 28	490 ± 31**
Serum glucose (mg/dL)	222.9 ± 110.0	275.1 ± 121.4	284.0 ± 84.1	259.7 ± 108.9
Serum ALT (IU/L)	15.5 ± 6.5	30.6 ± 38.1	21.8 ± 11.4	281.2 ± 165.1***
Serum triglyceride (mg/dL)	99.9 ± 9.7	78.9 ± 10.8	98.3 ± 11.4	89.7 ± 13.3
Serum leptin (ng/mL)	0.45 ± 0.14	1.31 ± 0.31*	0.65 ± 0.22	1.60 ± 0.28**

Data are mean ± standard deviation.
*$P < 0.05$ compared with sham-operated non-transgenic mice. **$P < 0.05$ compared with sham-operated transgenic mice. ***$P < 0.01$ compared with mice in the other three groups.
ALT, alanine aminotransferase; OVX, ovariectomized.

results for hepatic steatosis. Thus, the increase in the serum ALT level in the OVX transgenic mice was thought to reflect the hepatic steatosis.

Ovariectomy increased ROS and IL-6 production in the liver

Only OVX transgenic mice showed marked hepatic steatosis, regardless of the comparable diet intake and the ratio of liver to bodyweight of OVX non-transgenic mice (Table 1). We have previously demonstrated that iron-overloaded male FL-N/35 transgenic mice expressing the HCV polyprotein develop severe hepatic steatosis through increased ROS production.[11] Therefore, we examined whether ROS production was relevant to the marked hepatic steatosis observed in the OVX transgenic mice. Ovariectomy significantly increased ROS (super-

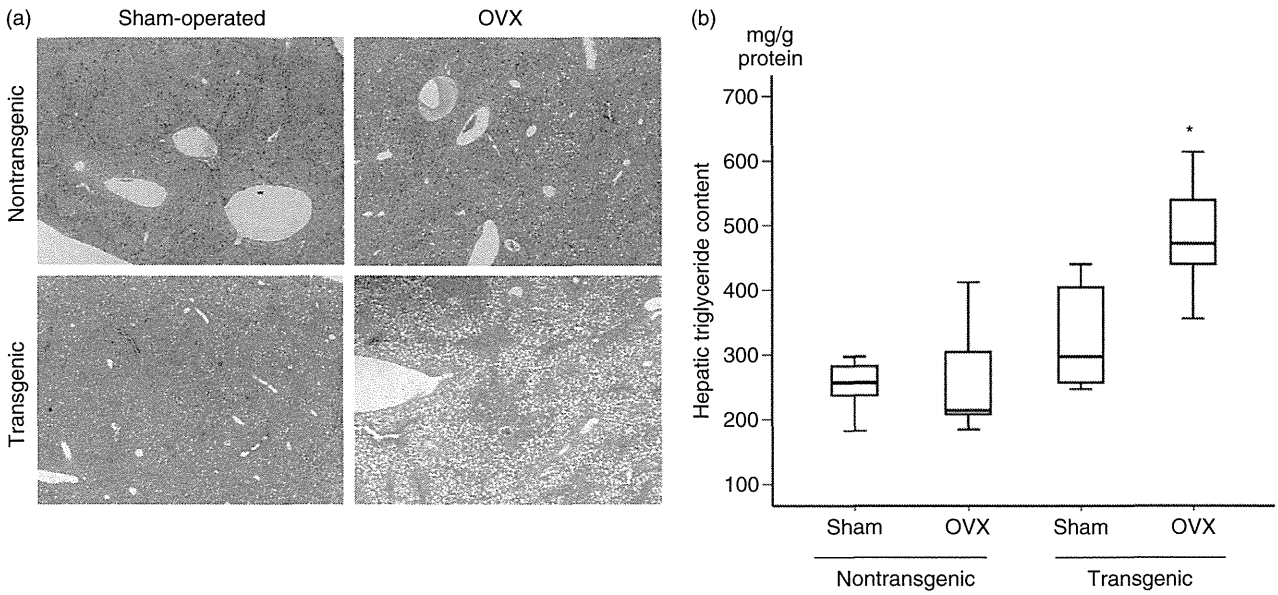

Figure 1 Hepatic steatosis and triglyceride content in sham-operated and ovariectomized (OVX) FL-N/35 transgenic and non-transgenic mice. (a) Hepatic steatosis in mice in each group (H&E, original magnification × 100). (b) Hepatic triglyceride content in mice in each group ($n = 5$). The results are shown as box plot profiles. The bottom and top edges of the boxes are the 25th and 75th percentiles, respectively. Median values are shown by the line within each box. *: $P < 0.05$ versus mice in the other three groups.

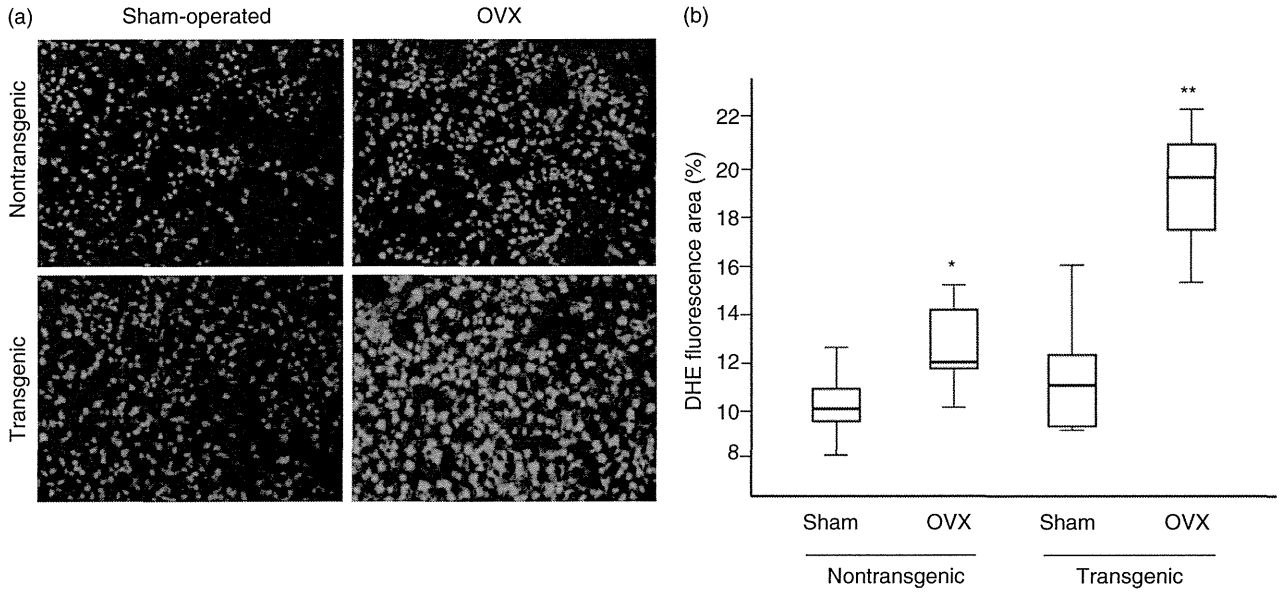

Figure 2 Reactive oxygen species (ROS) production in sham-operated and ovariectomized (OVX) FL-N/35 transgenic and non-transgenic mice. (a) Frozen liver sections from mice in each group were stained with dihydroethidium (DHE). (b) Fluorescence intensity was quantified by NIH image analysis software for three randomly selected areas of digital images for five mice in each group. The results are shown as box plot profiles. The bottom and top edges of the boxes are the 25th and 75th percentiles, respectively. Median values are shown by the line within each box. *: $P < 0.05$ versus sham-operated non-transgenic mice. **: $P < 0.05$ versus sham-operated nontransgenic mice, OVX non-transgenic mice and sham-operated transgenic mice.

oxide) production in both transgenic mice and non-transgenic mice, but the level of ROS production was greater in the OVX transgenic mice than in the OVX non-transgenic mice (Fig. 2). We next measured inflammatory cytokine levels in the liver. Ovariectomy significantly increased hepatic expression of IL-6 mRNA to the same degree in both transgenic mice and non-transgenic mice (Fig. 3). This ovariectomy-induced increase in hepatic IL-6 mRNA was consistent with the results of a previous report that OVX mice produced more hepatic

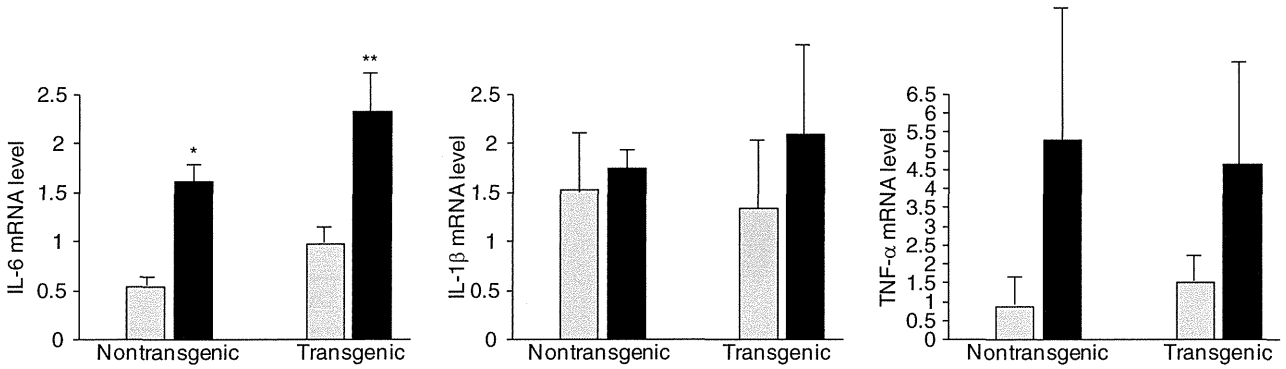

Figure 3 Expression levels of inflammatory cytokines in sham-operated and ovariectomized (OVX) FL-N/35 transgenic and non-transgenic mice. The mRNA levels of interleukin (IL)-6, IL-1β and tumor necrosis factor (TNF)-α were measured by real-time reverse transcription polymerase chain reaction for five mice in each group. The relative quantities of target mRNA in the liver were normalized with GAPDH mRNA. *$P < 0.05$ vs sham-operated non-transgenic mice. **$P < 0.05$ vs sham-operated transgenic mice. □, Sham; ■, OVX.

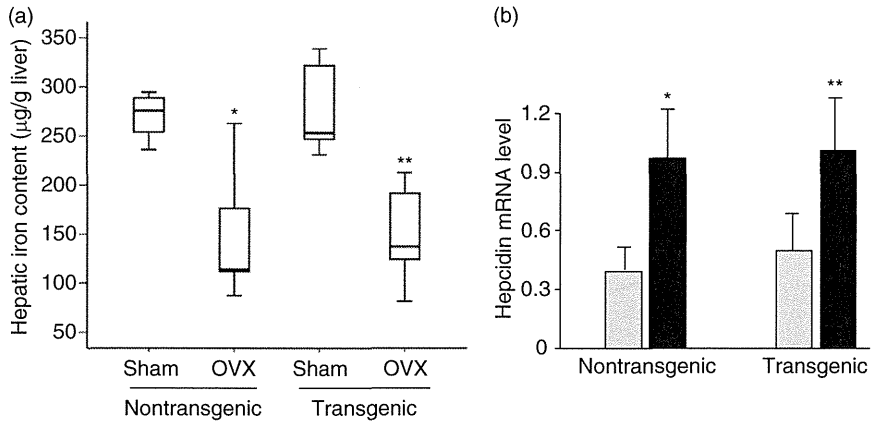

Figure 4 Hepatic iron content and hepcidin mRNA level in sham-operated and ovariectomized (OVX) FL-N/35 transgenic and non-transgenic mice. (a) Hepatic iron content in mice in each group ($n = 5$). The results are shown as box plot profiles. The bottom and top edges of the boxes are the 25th and 75th percentiles, respectively. Median values are shown by the line within each box. $^*P < 0.05$ vs sham-operated non-transgenic mice. $^{**}P < 0.05$ vs sham-operated transgenic mice. (b) The mRNA level of hepcidin was measured by real-time reverse transcription polymerase chain reaction for five mice in each group. The relative quantities of target mRNA in the liver were normalized with GAPDH mRNA. $^*P < 0.05$ vs sham-operated non-transgenic mice. $^{**}P < 0.05$ vs sham-operated transgenic mice. □, Sham; ■, OVX.

IL-6 than non-OVX mice after chemically induced liver injury.[5] There also was a trend for increase in TNF-α and IL-1β mRNA expression after ovariectomy in both the transgenic mice and non-transgenic mice, but their increases did not reach statistical significance, probably because of the large deviation (Fig. 3). These results suggested that inflammatory cytokines were unlikely to be associated with greater ROS production in OVX transgenic mice than in OVX non-transgenic mice.

Hepatic iron content and hepcidin expression level in the liver

We previously reported that male FL-N/35 transgenic mice developed hepatic iron accumulation through the reduced transcription of hepcidin,[18] a negative regulator in iron homeostasis.[21,22] Excess divalent iron can be highly toxic, mainly via the Fenton reaction producing hydroxyl radicals.[23] Therefore, we measured hepatic iron content to assess whether greater ROS production resulted from increased hepatic iron accumulation in OVX transgenic mice. Unexpectedly, ovariectomy significantly decreased hepatic iron content to the same degree in both transgenic mice and non-transgenic mice (Fig. 4a). These results are potentially explained by significantly increased transcription of hepcidin after ovariectomy (Fig. 4b). Ovariectomy-induced increase in hepatic IL-6 mRNA may in turn account for increased hepcidin transcription, because IL-6 acts to stimulate hepcidin expression through the STAT3 pathway.[24] These results suggested that hepatic iron content was not related to greater ROS production in OVX transgenic mice than in OVX non-transgenic mice.

Attenuated antioxidant potential against ovariectomy-induced ROS production in FL-N/35 transgenic mice

The increase in inflammatory cytokine production and the hepatic iron content after ovariectomy were comparable in transgenic and non-transgenic mice. Nevertheless, the serum ALT level, hepatic steatosis and ROS production were greater in OVX transgenic mice than in OVX non-transgenic mice. Therefore we measured dROM and BAP in serum to compare antioxidant potentials in OVX transgenic and OVX non-transgenic mice. We confirmed the significant negative correlation between the ratio of BAP to dROM and hepatic content of superoxide (Fig. 5). As expected, the values for dROM were higher in OVX mice than in sham-operated mice, regardless of whether they were transgenic or non-transgenic. However, a significant increase in the BAP value was found in OVX non-transgenic mice but not in OVX transgenic mice, which resulted in a lower ratio of BAP to dROM in the OVX transgenic mice than in the OVX non-transgenic mice (Table 2).

The first line of defense against ROS is the detoxifying enzymes that scavenge ROS. These include SOD and

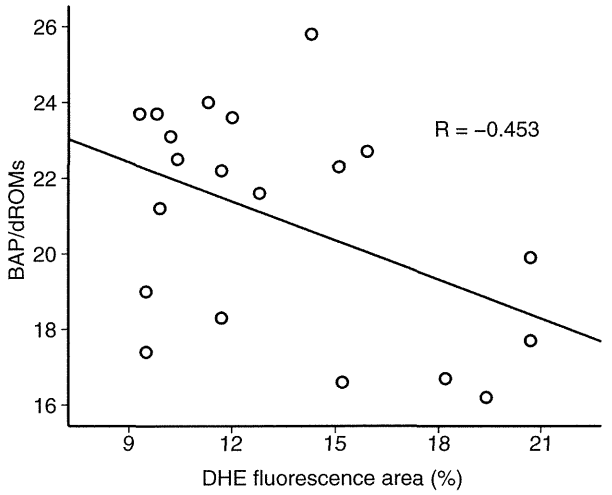

Figure 5 Negative correlation between the ratio of biological antioxidant potential (BAP) to derivatives of reactive oxygen metabolites (dROM) and hepatic content of superoxide. $R = -0.453$, $P < 0.05$. Hepatic content of superoxide was determined based on the area of dihydroethidium (DHE) fluorescence.

GPx1. Therefore we next investigated the expression levels of SOD2 and GPx1. The hepatic expression levels of SOD2 mRNA and GPx1 mRNA were significantly greater in OVX non-transgenic mice than in sham-operated non-transgenic mice, but were comparable in OVX transgenic mice and sham-operated transgenic mice (Fig. 6a). Western blot analysis of the hepatic mitochondria fractions also showed significant increases of SOD2 and GPx1 expression in OVX non-transgenic mice but not in OVX transgenic mice (Fig. 6b). These results suggested that antioxidant defense mechanisms may be induced against ovariectomy-related ROS production in non-transgenic mice but not in transgenic mice.

SIRT3 and PGC-1α expression in OVX FL-N/35 transgenic mice

Proliferator-activated receptor-γ co-activator-1α is a master regulator of mitochondrial biogenesis and respiration[25] and required for the induction of many ROS-detoxifying enzymes, including SOD2 and GPx1 upon oxidative stress.[26] SIRT3 is a member of a class III histone deacetylase and is reported to mediate PGC-1α-dependent induction of ROS-detoxifying enzymes.[27] In accordance with the changes in SOD2 and GPx1 levels after ovariectomy, the hepatic expression of SIRT3 mRNA was significantly greater in OVX non-transgenic mice than in sham-operated non-transgenic mice, but comparable in OVX transgenic mice and sham-operated transgenic mice (Fig. 7a). Western blot analysis of hepatic mitochondria showed a significant increase of SIRT3 expression in OVX non-transgenic mice but not in OVX transgenic mice (Fig. 7a).

Proliferator-activated receptor-γ co-activator-1α interacts with various nuclear receptors in addition to peroxisome proliferator-activated receptor-γ and is docked to the promoter of its target genes by all these nuclear receptors. Therefore, we investigated PGC-1α expression levels not only in liver homogenates but also in the nuclear fraction of mouse liver. The expression levels of PGC-1α in liver homogenates were comparable in sham-operated and OVX non-transgenic mice and in sham-operated and OVX transgenic mice. However, the expression levels of PGC-1α in the nuclear fraction of the liver significantly increased after ovariectomy in both non-transgenic and transgenic mice, and OVX transgenic mice had a lower PGC-1α expression level than OVX non-transgenic mice (Fig. 7b). These results suggested that the antioxidant potential against ovariectomy-induced ROS production may be reduced in OVX transgenic mice through lesser activation of PGC-1α than in OVX non-transgenic mice.

Table 2 Derivatives of reactive oxygen metabolites (dROM), biological antioxidant potential (BAP) and ratio of BAP to dROM

	Non-transgenic		Transgenic	
	Sham-operated	OVX	Sham-operated	OVX
dROM (U.CARR)	145.2 ± 15.1	158.7 ± 15.9*	170.8 ± 10.4	199.3 ± 21.1**
BAP (μmol/L)	3217 ± 123	3644 ± 177*	3362 ± 178	3542 ± 140
Ratio of BAP to dROM	22.3 ± 2.3	23.1 ± 2.0	20.8 ± 1.8	17.8 ± 1.9***

Data are mean ± standard deviation.
*$P < 0.05$ compared with sham-operated non-transgenic mice. **$P < 0.05$ compared with sham-operated transgenic mice. ***$P < 0.05$ compared with ovariectomized (OVX) non-transgenic mice.

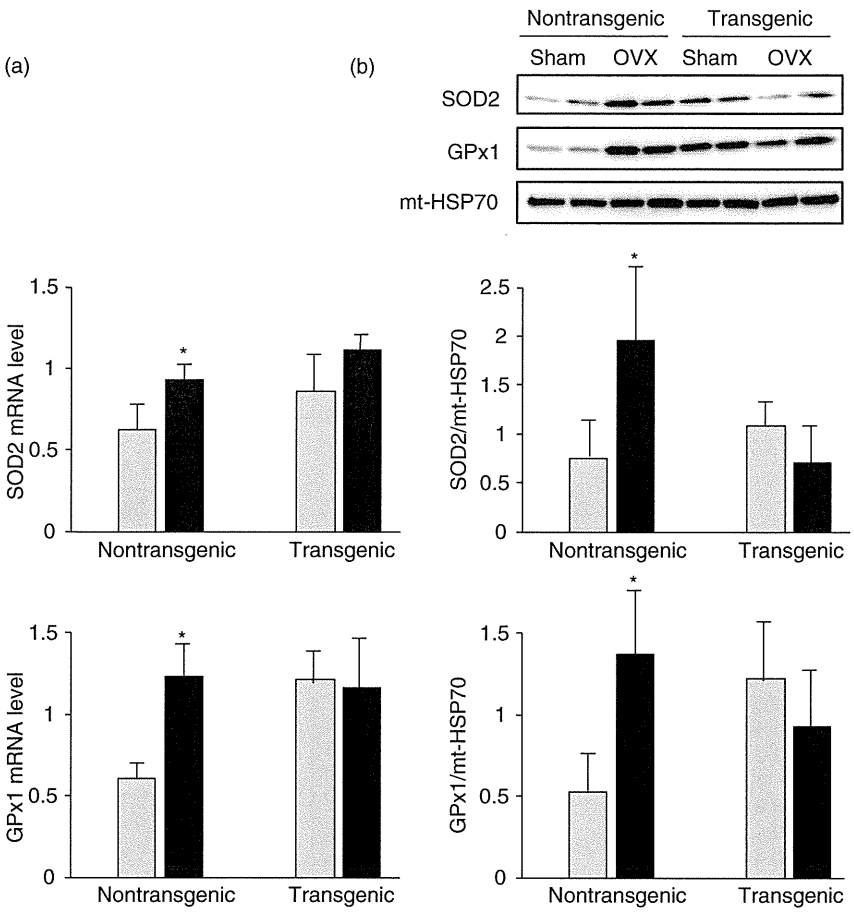

Figure 6 Expression levels of superoxide dismutase 2 (SOD2) and glutathione peroxidase 1 (GPx1) in sham-operated and ovariectomized (OVX) FL-N/35 transgenic and non-transgenic mice. (a) The mRNA levels of SOD2 and GPx1 were measured by real-time reverse transcription polymerase chain reaction for five mice in each group. The relative quantities of target mRNA in the liver were normalized with GAPDH mRNA. (b) Immunoblots for SOD2 and GPx1 were performed using mitochondrial fractions of liver lysates from five mice in each group. $^*P < 0.05$ vs sham-operated non-transgenic mice. □, Sham; ■, OVX.

Suppressed AMPK activation in OVX FL-N/35 transgenic mice

Proliferator-activated receptor-γ co-activator-1α activity is modulated through both transcriptional regulation and regulation of its activity by post-translational modifications.[28] AMPK is one of the signaling pathways regulating PGC-1α and acts both through modulation of PGC-1α transcription and by phosphorylation of the PGC-1α protein.[28] HCV has been shown to reduce the kinase activity of AMPK through Ser485/491 phosphorylation of AMPK.[29] Therefore, we examined the expression levels of AMPK to investigate the mechanisms underlying the lower PGC-1α expression in the nuclear fraction of the OVX transgenic liver. The expression levels of AMPKα, which is one of the three subunits (α, β and γ) of AMPK, were comparable in sham-operated and OVX mice and in non-transgenic and transgenic mice. However, the expression level of phosphorylated AMPKα was significantly greater in OVX non-transgenic mice than in mice in the three other groups, though it was similar in sham-operated transgenic mice and OVX transgenic mice (Fig. 7c). In addition, its levels were significantly greater in non-transgenic mice than in transgenic mice (Fig. 7c). These results suggested that AMPK was activated in OVX non-transgenic mice, but not in OVX transgenic mice, because AMPK is active only after phosphorylation of the α-subunit at a threonine residue within the kinase domain (T172) by upstream kinases.[30] Taken together, the results in the present study suggested that OVX FL-N/35 transgenic mice developed marked hepatic steatosis concomitant with increased ROS production via attenuation of antioxidant potential through inactivation of the AMPK/PGC-1α signaling pathway.

DISCUSSION

THE OVX MICE in the present study were assumed to be a standard model for evaluating the biological effect of ovariectomy because the effects of ovariectomy

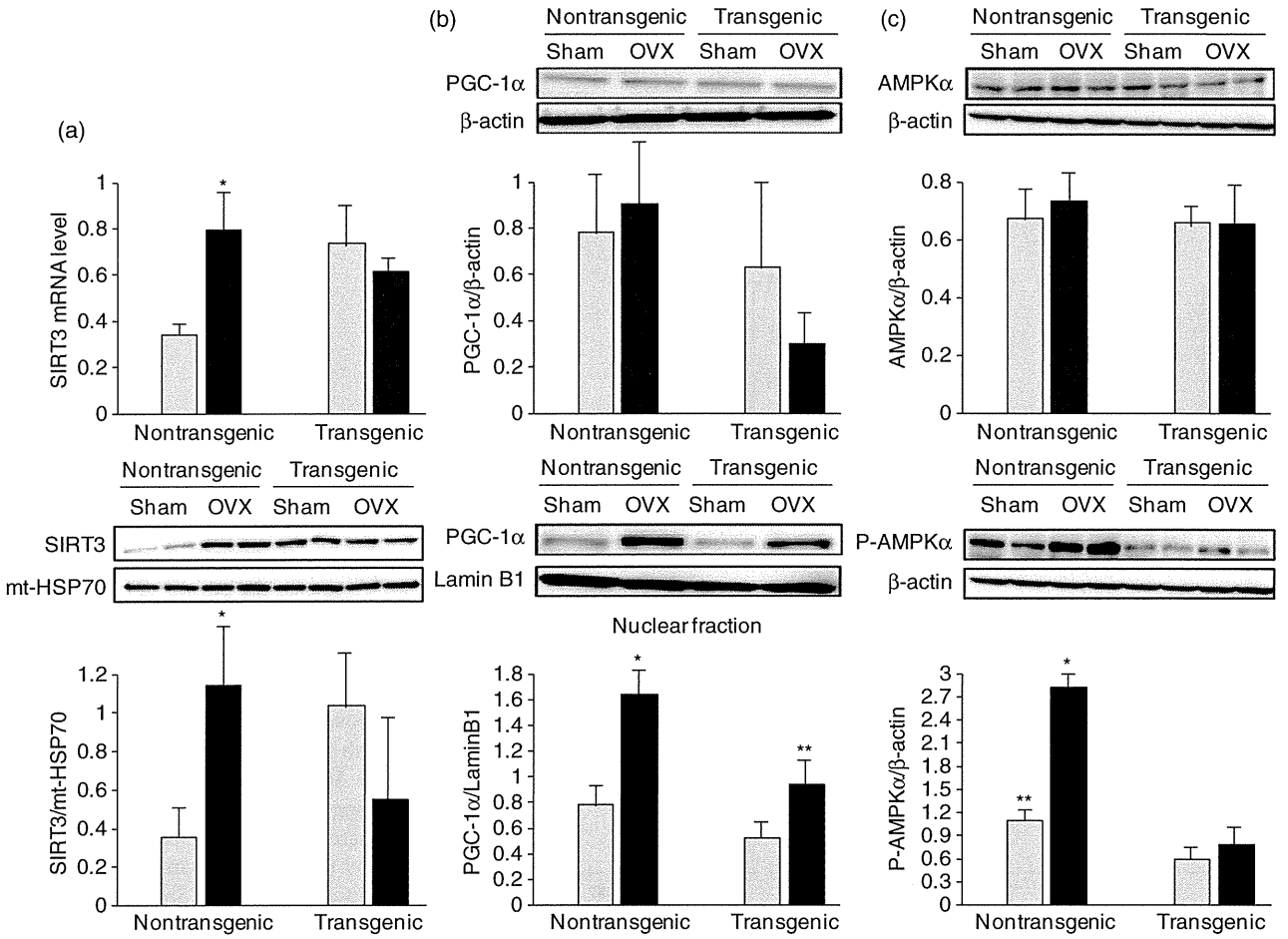

Figure 7 Expression levels of sirtuin 3 (SIRT3), peroxisome proliferator-activated receptor-γ co-activator-1α (PGC-1α), adenosine monophosphate-activated protein kinase α (AMPKα), and phosphorylated AMPKα (P-AMPKα) in sham-operated and ovariectomized (OVX) FL-N/35 transgenic and non-transgenic mice. (a) The mRNA levels of SIRT3 were measured by real-time reverse transcription polymerase chain reaction for five mice in each group. The relative quantities of target mRNA in the liver were normalized with GAPDH mRNA. Immunoblots for SIRT3 were performed using the mitochondrial fractions of liver lysates from five mice in each group. (b) Immunoblots for PGC-1α were performed using liver lysates and their nuclear fractions from five mice in each group. $*P < 0.05$ vs mice in the other three groups. $**P < 0.05$ vs sham-operated transgenic mice. (c) Immunoblots for AMPKα and P-AMPKα were performed using liver lysates from five mice in each group. $*P < 0.05$ vs mice in the other three groups. $**P < 0.05$ vs sham-operated transgenic mice. □, Sham; ■, OVX.

on dietary intake, bodyweight, uterine weight, liver weight and serum leptin levels were similar to the results from previous studies.[31–34] Ovariectomy increased ROS (superoxide) production in both transgenic liver and in non-transgenic liver, which was consistent with the ovariectomy-induced increase in NADPH oxidase activity[12] and the protective effect of estrogen against mitochondrial oxidative damage[13] found in previous studies. Of note was the much greater degree of ROS production after ovariectomy in transgenic mice than in non-transgenic mice. These results suggested that HCV protein expression has the potential to increase the sensitivity to oxidative stress in the liver. At least two possibilities may account for the increased sensitivity to oxidative stress in FL-N/35 transgenic mice. One possibility is an additive effect of HCV-induced ROS production on ovariectomy-induced oxidative stress. The HCV core protein has been shown to inhibit mitochondrial electron transport[35] and to induce ROS production.[36] In fact, basal ROS production tended to be higher in

transgenic mice than in non-transgenic mice, but was not significantly different. These results suggested that additive HCV-induced ROS production was unlikely to be the cause of the significantly increased ROS production after ovariectomy in the transgenic mice. The other possibility is HCV-associated attenuation of antioxidant potential against ovariectomy-induced oxidative stress. In this respect, OVX transgenic mice had a lower ratio of BAP to dROM than OVX non-transgenic mice and the expression of SOD2 and GPx1 in the liver was not increased. These results suggest that HCV protein attenuated antioxidant potential against ovariectomy-induced oxidative stress.

Proliferator-activated receptor-γ co-activator-1α is required for the induction of many ROS-detoxifying enzymes upon oxidative stress.[26] SIRT3 has been shown to function as a downstream target gene of PGC-1α and mediate the PGC-1α-dependent induction of ROS-detoxifying enzymes.[27] Additionally, AMPK, which is a crucial cellular energy sensor, regulates PGC-1α activity through both modulation of PGC-1α transcription and phosphorylation of the PGC-1α protein.[28,37] Thus, AMPK/PGC-1α signaling is one of the important pathways that protect cells from oxidative stress through the induction of several key ROS-detoxifying enzymes. Recent evidence indicating that HCV replication inhibits AMPK activity[29] prompted us to investigate whether the antioxidant potential against ovariectomy-induced oxidative stress in FL-N/35 transgenic mice was attenuated through inhibition of this signaling pathway. As expected, upon ovariectomy, AMPK was activated in non-transgenic mice, but not in transgenic mice. This, in turn, led to the lower expression of PGC-1α in the nuclear fraction of the liver in OVX transgenic mice than in OVX non-transgenic mice, resulting in the absence of significant induction of SIRT3 in the mitochondrial fraction of the liver in the OVX transgenic mice. Thus, ROS production in the liver in OVX transgenic mice was increased by attenuation of the antioxidant potential through inhibition of AMPK/PGC-1α signaling. However, it remains unknown why the expression of PGC-1α in the nuclear fraction was significantly increased in OVX transgenic mice regardless of the lack of activation of AMPK. Various kinases other than AMPK and post-translational modifications other than phosphorylation have been shown to regulate PGC-1α expression.[28] Therefore further investigations are required to clarify this issue.

Of particular concern is the relevance of the present results to HCC development in patients with HCV-associated chronic liver diseases. A recent study from Japan demonstrated a higher proportion of females, especially among elderly patients with HCV-related HCC, suggesting that the sex disparity in HCC development becomes less distinct as the patient's age at HCC diagnosis increases.[6] In general, ROS production creates a pro-carcinogenic environment under which chromosomal damage is likely to occur. The present findings that OVX transgenic mice have increased hepatic ROS production compared with that in OVX non-transgenic mice may indicate one of the mechanisms by which women with HCV infection are at high risk for HCC development when some period has passed after menopause, even though we need to clinically ascertain the increased hepatic oxidative stress in HCV-infected menopausal women with HCC.

ACKNOWLEDGMENTS

THIS RESEARCH WAS supported by a Grant-in-Aid for Scientific Research (B) (no. 23390201) and a Grant-in-aid for Exploratory Research (no. 25670374) from the Japan Society for the Promotion of Science, a Health and Labor Sciences Research Grant for Research on Hepatitis from the Ministry of Health, Labor and Welfare of Japan, and Research Project Grant P2 from Kawasaki Medical School.

REFERENCES

1 Chen DS, Locarnini S, Wait S *et al.* Report from a Viral Hepatitis Policy Forum on implementing the WHO framework for global action on viral hepatitis in North Asia. *J Hepatol* 2013. doi: 10.1016/j.jhep.2013.06.029.
2 Bruno S, Silini E, Crosignani A *et al.* Hepatitis C virus genotypes and risk of hepatocellular carcinoma in cirrhosis: a prospective study. *Hepatology* 1997; **25**: 754–8.
3 Degos F, Christidis C, Ganne-Carrie N *et al.* Hepatitis C virus related cirrhosis: time to occurrence of hepatocellular carcinoma and death. *Gut* 2000; **47**: 131–6.
4 Bosch FX, Ribes J, Diaz M, Cleries R. Primary liver cancer: worldwide incidence and trends. *Gastroenterology* 2004; **127**: S5–S16.
5 Naugler WE, Sakurai T, Kim S *et al.* Gender disparity in liver cancer due to sex differences in MyD88-dependent IL-6 production. *Science* 2007; **317**: 121–4.
6 Kumada T, Toyoda H, Kiriyama S *et al.* Characteristics of elderly hepatitis C virus-associated hepatocellular carcinoma patients. *J Gastroenterol Hepatol* 2013; **28**: 357–64.
7 Farinati F, Cardin R, De Maria N *et al.* Iron storage, lipid peroxidation and glutathione turnover in chronic anti-HCV positive hepatitis. *J Hepatol* 1995; **22**: 449–56.
8 Barbaro G, Di Lorenzo G, Asti A *et al.* Hepatocellular mitochondrial alterations in patients with chronic hepatitis C:

ultrastructural and biochemical findings. *Am J Gastroenterol* 1999; **94:** 2198–205.
9 Tanaka H, Fujita N, Sugimoto R *et al.* Hepatic oxidative DNA damage is associated with increased risk for hepatocellular carcinoma in chronic hepatitis C. *Br J Cancer* 2008; **98:** 580–6.
10 Moriya K, Nakagawa K, Santa T *et al.* Oxidative stress in the absence of inflammation in a mouse model for hepatitis C virus-associated hepatocarcinogenesis. *Cancer Res* 2001; **61:** 4365–70.
11 Furutani T, Hino K, Okuda M *et al.* Hepatic iron overload induces hepatocellular carcinoma in transgenic mice expressing the hepatitis C virus polyprotein. *Gastroenterology* 2006; **130:** 2087–98.
12 Ji H, Zheng W, Menini S *et al.* Female protection in progressive renal disease is associated with estradiol attenuation of superoxide production. *Gend Med* 2007; **4:** 56–71.
13 Borras C, Sastre J, Garcia-Sala D, Lloret A, Pallardo FV, Vina J. Mitochondria from females exhibit higher antioxidant gene expression and lower oxidative damage than males. *Free Radic Biol Med* 2003; **34:** 546–52.
14 Beard MR, Abell G, Honda M *et al.* An infectious molecular clone of a Japanese genotype 1b hepatitis C virus. *Hepatology* 1999; **30:** 316–24.
15 Lerat H, Honda M, Beard MR *et al.* Steatosis and liver cancer in transgenic mice expressing the structural and nonstructural proteins of hepatitis C virus. *Gastroenterology* 2002; **122:** 352–65.
16 Bligh EG, Dyer WJ. A rapid method of total lipid extraction and purification. *Can J Biochem Physiol* 1959; **37:** 911–7.
17 Lowry OH, Rosebrough NJ, Farr AL, Randall RJ. Protein measurement with the Folin phenol reagent. *J Biol Chem* 1951; **193:** 265–75.
18 Nishina S, Hino K, Korenaga M *et al.* Hepatitis C virus-induced reactive oxygen species raise hepatic iron level in mice by reducing hepcidin transcription. *Gastroenterology* 2008; **134:** 226–38.
19 Harrison-Findik DD, Schafer D, Klein E *et al.* Alcohol metabolism-mediated oxidative stress down-regulates hepcidin transcription and leads to increased duodenal iron transporter expression. *J Biol Chem* 2006; **281:** 22974–82.
20 Cesarone MR, Belcaro G, Carratelli M *et al.* A simple test to monitor oxidative stress. *Int Angiol* 1999; **18:** 127–30.
21 Park CH, Valore EV, Waring AJ, Ganz T. Hepcidin, a urinary antimicrobial peptide synthesized in the liver. *J Biol Chem* 2001; **276:** 7806–10.
22 Nemeth E, Tuttle MS, Powelson J *et al.* Hepcidin regulates cellular iron efflux by binding to ferroportin and inducing its internalization. *Science* 2004; **306:** 2090–3.
23 Fenton HJH. Oxidation of tartaric acid in presence of iron. *J Chem Soc* 1894; **65:** 899–910.
24 Pietrangelo A, Dierssen U, Valli L *et al.* STAT3 is required for IL-6-gp130-dependent activation of hepcidin in vivo. *Gastroenterology* 2007; **132:** 294–300.
25 Kelly DP, Scarpulla RC. Transcriptional regulatory circuits controlling mitochondrial biogenesis and function. *Genes Dev* 2004; **18:** 357–68.
26 St-Pierre J, Drori S, Uldry M *et al.* Suppression of reactive oxygen species and neurodegeneration by the PGC-1 transcriptional coactivators. *Cell* 2006; **127:** 397–408.
27 Kong X, Wang R, Xue Y *et al.* Sirtuin 3, a new target of PGC-1alpha, plays an important role in the suppression of ROS and mitochondrial biogenesis. *PLoS ONE* 2010; **5:** e11707.
28 Fernandez-Marcos PJ, Auwerx J. Regulation of PGC-1alpha, a nodal regulator of mitochondrial biogenesis. *Am J Clin Nutr* 2011; **93:** 884S–90.
29 Mankouri J, Tedbury PR, Gretton S *et al.* Enhanced hepatitis C virus genome replication and lipid accumulation mediated by inhibition of AMP-activated protein kinase. *Proc Natl Acad Sci U S A* 2010; **107:** 11549–54.
30 Hawley SA, Boudeau J, Reid JL *et al.* Complexes between the LKB1 tumor suppressor, STRAD alpha/beta and MO25 alpha/beta are upstream kinases in the AMP-activated protein kinase cascade. *J Biol* 2003; **2:** 28.
31 Rogers NH, Perfield JW 2nd, Strissel KJ, Obin MS, Greenberg AS. Reduced energy expenditure and increased inflammation are early events in the development of ovariectomy-induced obesity. *Endocrinology* 2009; **150:** 2161–8.
32 Pighon A, Gutkowska J, Jankowski M, Rabasa-Lhoret R, Lavoie JM. Exercise training in ovariectomized rats stimulates estrogenic-like effects on expression of genes involved in lipid accumulation and subclinical inflammation in liver. *Metabolism* 2011; **60:** 629–39.
33 Hong J, Stubbins RE, Smith RR, Harvey AE, Nunez NP. Differential susceptibility to obesity between male, female and ovariectomized female mice. *Nutr J* 2009; **8:** 11.
34 Kamada Y, Kiso S, Yoshida Y *et al.* Pitavastatin ameliorated the progression of steatohepatitis in ovariectomized mice fed a high fat and high cholesterol diet. *Hepatol Res* 2013; **43:** 401–12.
35 Korenaga M, Wang T, Li Y *et al.* Hepatitis C virus core protein inhibits mitochondrial electron transport and increases reactive oxygen species (ROS) production. *J Biol Chem* 2005; **280:** 37481–8.
36 Okuda M, Li K, Beard MR *et al.* Mitochondrial injury, oxidative stress, and antioxidant gene expression are induced by hepatitis C virus core protein. *Gastroenterology* 2002; **122:** 366–75.
37 Hardie DG, Ross FA, Hawley SA. AMPK: a nutrient and energy sensor that maintains energy homeostasis. *Nat Rev Mol Cell Biol* 2012; **13:** 251–62.

Hepatology Research

Hepatology Research 2014 doi: 10.1111/hepr.12247

Review Article

Mitochondrial reactive oxygen species as a mystery voice in hepatitis C

Keisuke Hino, Yuichi Hara and Sohji Nishina

Department of Hepatology and Pancreatology, Kawasaki Medical School, Kurashiki, Japan

There are several lines of evidence suggesting that oxidative stress is present in hepatitis C to a greater degree than in other inflammatory liver diseases and is closely related to disease progression. The main production site of reactive oxygen species (ROS) is assumed to be mitochondria, which concept is supported by evidence that hepatitis C virus (HCV) core protein is directly associated with them. The detoxification of ROS also is an important function of the cellular redox homeostasis system. These results draw our attention to how HCV-induced mitochondrial ROS production is beyond redox regulation and affects the disease progression and development of hepatocellular carcinoma (HCC) in chronic hepatitis C. On the other hand, HCV-related chronic liver diseases are characterized by metabolic alterations such as insulin resistance, hepatic steatosis and/or iron accumulation in the liver. These metabolic disorders also are relevant to the development of HCC in HCV-related chronic liver diseases. Here, we review the mechanisms by which HCV increases mitochondrial ROS production and offer new insights as to how mitochondrial ROS are linked to metabolic disorders such as insulin resistance, hepatic steatosis and hepatic iron accumulation that are observed in HCV-related chronic liver diseases.

Key words: calcium signaling, mitochondrial electron transport, mitophagy, hepcidin, insulin resistance, iron metabolism

INTRODUCTION

APPROXIMATELY 170 MILLION people worldwide are infected with hepatitis C virus (HCV).[1] HCV infection often remains asymptomatic, but can lead to chronic hepatitis, cirrhosis and hepatocellular carcinoma (HCC).[2] Although the mechanisms of its pathogenesis are incompletely understood, there are several lines of evidence suggesting that oxidative stress is present in hepatitis C to a greater degree than in other inflammatory liver diseases and is closely related to disease progression.[3–6] Previous *in vitro* and *in vivo* studies have shown that HCV core protein induces the production of reactive oxygen species (ROS)[7–9] and that mitochondrial electron transport inhibition by HCV core protein is associated with ROS production.[10,11] These results draw our attention to how HCV-induced mitochondrial injury contributes to disease progression and hepatocarcinogenesis in hepatitis C.

On the other hand, HCV-related chronic liver diseases are characterized by metabolic alterations such as insulin resistance,[12–14] hepatic steatosis[15,16] and/or iron accumulation in the liver.[3,17] These metabolic disorders also are relevant to the development of HCC in HCV-related chronic liver diseases.[18–21] The present review highlights the mechanisms underlying the production of mitochondrial ROS by HCV and the metabolic disorders induced by mitochondrial dysfunction, and discuss how mitochondrial ROS contribute to the disease progression and hepatocarcinogenesis in hepatitis C.

Correspondence: Professor Keisuke Hino, Department of Hepatology and Pancreatology, Kawasaki Medical School, 577 Matsushima, Kurashiki, Okayama 701-0192, Japan. Email: khino@med.kawasaki-m.ac.jp

Received 25 May 2013; revision 5 September 2013; accepted 19 September 2013.

MITOCHONDRIAL ROS PRODUCTION

Mitochondrial electron transport and ROS production

THE MITOCHONDRIAL ELECTRON transport system consists of several multi-polypeptide protein complexes (I–V) embedded in the inner mitochondrial membrane that receive electrons from reducing equivalents (i.e. nicotinamide adenine dinucleotide and

$FADH_2$) generated by dehydrogenases (e.g. pyruvate dehydrogenase, α-ketoglutarate dehydrogenase, acyl-coenzyme A dehydrogenase). These electrons flow through complex I, the ubiquinone cycle (Q/QH_2), complex III, cytochrome c, complex IV, and to the final acceptor O_2 to form H_2O. Electron flow through complexes I, III and IV results in the pumping of protons to the outer surface of the inner membrane, establishing a membrane potential that is used by adenosine triphosphate synthetase to drive the re-phosphorylation of adenine dinucleotide phosphate. Several of the redox couples within the electron transport chain transfer single rather than two electrons and are therefore susceptible to leaking electrons directly to surrounding O_2 to form the free-radical superoxide ($O_2\bullet^-$). The detoxification of ROS is an important function of the cellular redox homeostasis system. Cells rapidly convert $O_2\bullet^-$ into the two-electron non-radical hydrogen peroxide (H_2O_2) by manganese superoxide dismutase (MnSOD). H_2O_2 in turn can be further reduced to H_2O in the mitochondrial matrix by glutathione (GSH) or the thioredoxin/peroxiredoxin systems, or can freely diffuse out of the mitochondria where it again is buffered by GSH.[22]

Interaction of HCV core protein with mitochondria and mitochondrial ROS production

Hepatitis C virus core protein has been shown to directly associate with mitochondria. While the initial reports showed that HCV core protein associated exclusively with the mitochondrial outer membrane via a C-terminal motif,[10,23] a recent study using electronic microscopy suggests that HCV core protein is also associated with the mitochondrial inner membrane.[24] Importantly, Schwer *et al.* have demonstrated that core protein associates with the mitochondria-associated membrane (MAM) fraction, a point of close contact between the endoplasmic reticulum (ER) and mitochondrion.[23] In addition, biochemical evidence suggests that the interaction also takes place in the context of productively replicative HCV in cell culture (HCVcc),[25] even though subcellular analysis using confocal microscopy did not confirm a direct interaction of the HCV core with mitochondria in HCVcc infected Huh7.5 cells.[26] Direct interaction of HCV core protein with mitochondria potentially modifies mitochondrial ROS production and scavenging, which subsequently induce oxidative stress. The effects of HCV on ROS production and scavenging are summarized in Table 1.[27] When mitochondrial electron transport activity is inhibited by HCV core protein,[10,28] electrons are likely to leak from the electron transport chain transfer, accelerating mitochondrial $O_2\bullet^-$ production and/or H_2O_2 emission. Induction of mitochondrial and/or cellular antioxidant enzymes concomitantly with ROS production may be explained by antioxidant defense mechanisms rather than direct induction of antioxidant enzymes by HCV, even though HCV core and non-structural proteins have been reported to lead to different effects on cellular

Table 1 Effects of HCV on ROS production or scavenging *in vitro* and *in vivo*

Effect on ROS production or scavenging	*In vitro* and *in vivo* HCV models	References
Inhibition of mitochondrial electron transport	Structural gene transgenic mice, core gene transgenic mice, full genomic replicon cells	10, 28
Oxidation of glutathione pool	Structural gene transgenic mice, core- and non-structural protein-expressing cell lines	10, 29
Induction of mitochondrial antioxidant enzymes	Non-structural protein-expressing cell lines	29
Inhibition of gastrointestinal-glutathione peroxidase	Subgenomic replicon cells	30
Induction of glutathione peroxidase	Core-expressing cell line, subgenomic replicon cells	8, 30
Oxidation of the thioredoxin pool	Core-expressing cell line	29
Increase in lipid peroxidation	Core-expressing cell line, core gene transgenic mice	8, 31
Induction of metallothionein	Core-expressing cell line	8, 32
Cytoplasmic ROS production by NADPH oxidase	Core-expressing cell line, subgenomic replicon cells, full genomic replicon cells, HCV-infected Huh7 cells (JFH)	33, 34

HCV, hepatitis C virus; NADPH, nicotinamide adenine dinucleotide phosphate; ROS, reactive oxygen species.

antioxidant defenses.[29] Thus, one of the major sources for intracellular ROS production by core protein is the mitochondrion, even though the core is also involved in ROS production at the plasma membrane by activating nicotinamide adenine dinucleotide phosphate oxidase 4.[33,34]

Modulated calcium signaling by HCV and mitochondrial ROS production

The close physical association between the ER and mitochondria mediated by MAM results in Ca^{2+} microdomains at contact points that facilitate efficient Ca^{2+} transmission from the ER to mitochondria.[35] Although sufficient intra-organelle Ca^{2+} concentrations are required to stimulate metabolism by activating enzymes critical for maintenance of the tricarboxylic acid (TCA) cycle,[36] prolonged increases of Ca^{2+} can, in turn, interfere with the activity of these enzymes. The TCA cycle activity affects the electron transport chain activity, which in turn affects the mitochondrial membrane potential ($\Delta\Psi$). Thus, increased Ca^{2+} influx to mitochondria induces a substrate imbalance of the TCA cycle that leads to the generation of mitochondrial ROS, probably through the inhibition of electron transport chain activity. There are several lines of evidence indicating that HCV increases mitochondrial ROS production by modulating calcium signaling.[37–39] The HCV NS5A protein is reported to cause a disturbance of intracellular Ca^{2+} signaling, which triggers mitochondrial ROS production.[37] As shown in Figure 1, HCV core protein also enhances mitochondrial Ca^{2+} uptake in response to ER Ca^{2+} release through activation of the mitochondrial Ca^{2+} uniporter, which leads to increased mitochondrial ROS production.[38,39] Pharmacological inhibition of ER–mitochondrial Ca^{2+} fluxes, but not ROS scavengers, has been shown to normalize all aberrant effects induced by HCV: normalization of the electron transport chain complex I activity, restoration of mitochondrial $\Delta\Psi$ and normalization of ROS concentrations. More importantly, the time course and titration of HCV polyprotein expression suggest that mitochondrial Ca^{2+} uptake is the earliest of these above events induced by HCV.[39] Thus, mitochondrial Ca^{2+} uptake may be the initial event associated with mitochondrial dysfunction induced by HCV and may, in turn, trigger complex I inhibition, loss of mitochondrial $\Delta\Psi$ and ROS production. All these effects could be counteracted by intracellular Ca^{2+} chelation, suggesting that control of mitochondrial Ca^{2+} uptake may be useful as a new therapeutic intervention.

MITOCHONDRIAL QUALITY CONTROL

AS MENTIONED ABOVE, the detoxification of ROS is an important function of the cellular redox homeostasis system. Under resting cellular conditions, the intracellular redox environment is in a relatively reduced state.[40] Therefore, the next question is how HCV core-induced mitochondrial ROS production and the subsequent oxidative stress persist in spite of the presence of ROS-detoxifying agents such as MnSOD and/or GSH or the thioredoxin/peroxiredoxin systems. There are several lines of evidence indicating that mitochondrial injury is present in patients with chronic hepatitis C[4] and transgenic mice expressing the HCV core protein.[19] Although it remains unknown whether damaged mitochondria behave as an active ROS source, they are assumed to have less ROS-detoxifying activity than intact mitochondria. In mammalian cells, the autophagy-dependent degradation of mitochondria (mitophagy) is thought to maintain mitochondrial quality by eliminating damaged mitochondria.[41,42] Indeed, mitophagy plays an essential role in reducing mitochondrial ROS production and mitochondrial DNA mutations in yeast.[43] Mitochondrial membrane depolarization precedes the induction of mitophagy,[44] which is selectively controlled by a variety of proteins in mammalian cells, including phosphatase and tensin homolog (PTEN)-induced kinase 1 (PINK1) and the E3 ubiquitin ligase Parkin.[41,45] PINK1 facilitates Parkin targeting to the depolarized mitochondria[45] and, although Parkin ubiquitinates a broad range of mitochondrial outer membrane proteins,[45] it remains unclear how Parkin enables damaged mitochondria to be recognized by the autophagosome. We recently found that HCV core protein suppresses mitophagy by inhibiting the translocation of Parkin to the mitochondria via a direct interaction with it (Yuichi Hara, unpubl. data, 2013). Considering that oxidative stress and/or hepatocellular mitochondrial alterations are present in chronic hepatitis C to a greater degree than in other inflammatory liver diseases[3–6] and that mitophagy is important for maintaining mitochondrial quality by eliminating damaged mitochondria, our finding that HCV core protein suppresses mitophagy may in part explain the pathophysiology of chronic hepatitis C. However, in contrast to our results, Siddiqui *et al.* have shown that HCV induces the mitochondrial translocation of Parkin and subsequent mitophagy.[46] In addition, their results indicated that the HCV-mediated decline of mitochondrial complex I enzyme activity was rescued by chemical inhibition of mitophagy or by Parkin silenc-

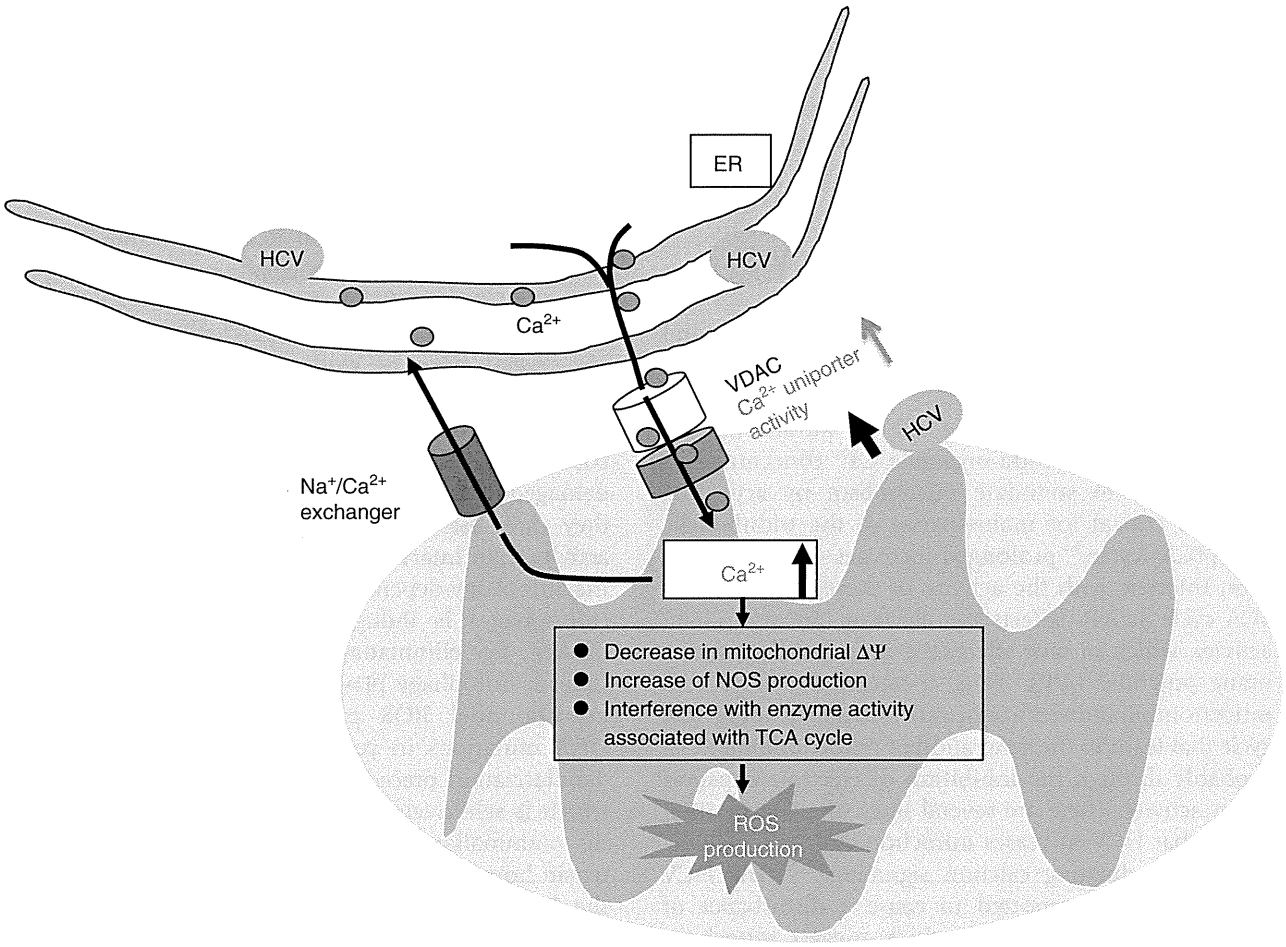

Figure 1 Schematic diagram depicting hepatitis C virus (HCV)-related calcium transfer from the endoplasmic reticulum (ER) to the mitochondria in the mitochondria-associated membrane (MAM) fraction. HCV core protein enhances mitochondrial Ca^{2+} uptake in response to ER Ca^{2+} release through activation of the mitochondrial Ca^{2+} uniporter, which leads to increased mitochondrial ROS production The voltage-dependent anion channel (VDAC) is the major component of the mitochondrial permeability transition (MPT) pore. It is assumed that there is spatial proximity of the complexes responsible for ER Ca^{2+} release, mitochondrial Ca^{2+} uptake and the MPT pore.

ing, and suggested that induction of mitophagy by HCV may significantly contribute to the mitochondrial injury associated with chronic hepatitis C. Thus, it still remains a matter of debate as to whether HCV induces or suppresses mitophagy and how oxidative stress persists in HCV infection.

METABOLIC ALTERATIONS BY MITOCHONDRIAL ROS

Insulin resistance

TYPE 2 DIABETES mellitus is one of the important extrahepatic manifestations associated with chronic HCV infection.[47,48] The final common pathway responsible for the development of type 2 diabetes mellitus is the failure of the pancreatic β-cells to compensate for insulin resistance. Although the molecular mechanisms by which HCV promotes insulin resistance have not been fully elucidated, there are several lines of evidence suggesting that HCV directly induces insulin resistance.[49–51] Insulin receptor substrate (IRS)1 and IRS2 are normally expressed in hepatocytes and central molecules of the hepatic insulin signal cascade. HCV core protein is reported to upregulate suppressor cytokine signal (SOCS)3 and cause ubiquitination of IRS1 and IRS2, leading to their proteosomal degradation.[50] SOCS3 also suppresses phosphorylation of tyrosine within IRS1.[52,53] Inhibition of tyrosine phos-